

## KARAMUSTAFA ALTIN İÇEREN Zn-Pb MADEN (GÜMÜŞHANE, TÜRKİYE) SAHASININ DOĞAL VE YAPAY RADYOAKTİVİTE AÇISINDAN İNCELENMESİ

**Alaaddin VURAL\***

Ankara University, Faculty of Engineering, Department of Geological Engineering, 06830 Gölbaşı/Ankara, Türkiye,  
[alaaddinvural@hotmail.com](mailto:alaaddinvural@hotmail.com), [0000-0002-0446-828X](tel:0000-0002-0446-828X)

**Ali KAYA**

Gümüşhane University, Faculty of Engineering and Natural Sciences, Department of Physics Eng. Gümüşhane,  
Türkiye, [alikaya@gumushane.edu.tr](mailto:alikaya@gumushane.edu.tr), [0000-0003-2326-0705](tel:0000-0003-2326-0705)

### Öz

Bu çalışma, özellikle baz metal içerikli maden yataklarının tıbbi jeoloji bağlamında doğal ve yapay radyoaktivite içeriklerinin çevresel etkilerinin incelenmesi amaçlamıştır. Çalışmayla Gümüşhane'nin (KD Türkiye) önemli madenlerinden biri olan Karamustafa altın içeren Zn-Pb-(±Cu) maden sahasının topraklarındaki yapay/antropojenik ( $^{137}\text{Cs}$ ) ve doğal ( $^{226}\text{Ra}$ ,  $^{232}\text{Th}$  ve  $^{40}\text{K}$ ) radyoaktivite seviyeleri belirlenmiş ve değerlendirilmiştir. Maden sahanın doğal ve yapay radyoaktivitelerini belirlemek için sahanın jeolojik ve alterasyon özellikleri dikkate alınarak, sahayı kapsayacak şekilde sahanın değişik kesimlerinden 9 adet toprak örneği toplanmıştır. İlgili laboratuvar prosedürlerine göre ile hazırlanan örneklerin gama-ışını spektrometresiyle  $^{232}\text{Th}$ ,  $^{226}\text{Ra}$  ve  $^{40}\text{K}$  aktiviteleri belirlenmiş, ayrıca  $^{137}\text{Cs}$ 'in yapay radyoaktivite değerleri de ölçülmüştür. Çalışma sonucunda, Karamustafa altın içeren Zn-Pb-(±Cu) maden sahasının ortalama  $^{40}\text{K}$  ve  $^{226}\text{Ra}$  aktivitelerinin örnek alım noktalarının büyük çoğunluğunda dünya ortalamalarını aştığı,  $^{232}\text{Th}$  aktivitelerinin ise bir kısım örnek alım noktalarında dünya ortalamasının üstünde olduğu belirlenmiştir. Sahadaki yapay/insan kaynaklı  $^{137}\text{Cs}$  radyoizotop değerlerinin de dikkat çekici oranda yüksek olduğu tespit edilmiştir. Saha için hesaplanmış belli başlı radio indeksler dikkate alındığında ise maden sahasının absorbe doz oranı ve yıllık efektif doz oranı indekslerinin ilgili eşik değerleri aştığı tespit edilmiştir. Sahaya ait elde edilen tüm veriler birlikte değerlendirildiğinde maden sahasının radyasyon riski bağlamında detaylı çalışmaya ihtiyaç duyduğu kanaatine varılmıştır.

**Anahtar Kelimeler:**  $^{226}\text{Ra}$ ,  $^{232}\text{Th}$ ,  $^{40}\text{K}$  Doğal radioizotopları,  $^{137}\text{Cs}$  Yapay radyoizotopu, Gümüşhane, Türkiye.

## ASSESSMENT OF KARAMUSTAFA GOLD-BEARING Zn-Pb MINE (GÜMÜŞHANE, TÜRKİYE) AREA IN TERMS OF NATURAL AND ARTIFICIAL RADIOACTIVITY

### Abstract

This study aimed to assess the environmental effects of natural and artificial radioactivity contents, especially in the context of medical geology of base metal-containing mineral deposits. In the study, artificial/anthropogenic ( $^{137}\text{Cs}$ ) and natural ( $^{226}\text{Ra}$ ,  $^{232}\text{Th}$  and  $^{40}\text{K}$ ) radioactivity levels in the soil of the Karamustafa gold-bearing Zn-Pb-(±Cu) mining area, one of the important mines of Gümüşhane (NE Türkiye), were determined and evaluated. In order to determine the natural and artificial radioactivity of the mining area, 9 soil samples were collected from different parts of the field, taking into account the geological and alteration characteristics of the field.  $^{232}\text{Th}$ ,  $^{226}\text{Ra}$  and  $^{40}\text{K}$  activities of the samples prepared according to the relevant laboratory procedures were determined by the gamma-ray spectrometry, and the artificial radioactivity values of  $^{137}\text{Cs}$  were also measured. As a result of the study, it was determined that the  $^{40}\text{K}$  and  $^{226}\text{Ra}$  average activities of the Karamustafa gold-bearing Zn-Pb-(±Cu) mining area exceeded the world averages in most sampling points, while the  $^{232}\text{Th}$  activities were above the world averages at some sampling points. It has been determined that the artificial/human-derived  $^{137}\text{Cs}$  radioisotope values in the field are remarkably high. Considering the major radio indices calculated for the field, it was determined that the absorbed dose rate and annual effective dose rate indices of the mine site exceeded the relevant threshold values. When all the data obtained from the field were evaluated together, it was concluded that the mine field needed detailed study in the context of radiation risk.

**Keywords:**  $^{226}\text{Ra}$ ,  $^{232}\text{Th}$ ,  $^{40}\text{K}$  Natural radioisotopes,  $^{137}\text{Cs}$  Artificial radioisotope, Gümüşhane, Türkiye.

## 1. INTRODUCTION

Nowadays, the concept of “natural” has become a fashionable term. The word, which is used as an adjective phrase in almost every word, has become a magic word. When the attribute natural is added, it is as if every commodity turns into a good/ideal. The natural nature of vegetables, the natural nature of fruits, the natural nature of the environment, in short, everything natural is accepted as acceptable. So, is everything natural good? Exemplifying this phenomenon, human beings are consistently and inherently subject to the influence of natural radiation throughout the entirety of their existence. The extent of radiation exposure varies, contingent upon the geographical location and the geological or geochemical attributes of the surrounding environment. Radiation emanates from radioactive nuclei intrinsic to the Earth's structure, cosmic radiation originating from the solar system, and additionally arises from anthropogenic activities induced by human endeavors. The interaction of human beings with their natural environment started with their existence on earth, and this interaction has been two-way, both in the form of benefiting from the earth's opportunities and in the form of an impact from this environment to humans (1, 2). These interactions, especially those from humans to nature, can be considered the beginning of small-scale environmental problems (3–6). Although studies on natural resources and environmental problems arising from the exploration and exploitation of these resources have increased in recent years (7–10), relatively few studies on the investigation of natural radiation activities of mineralization / mining areas that occur as a result of important geochemical and physicochemical processes have started to increase in recent years (11–16). In real terms, environmental problems and their global effects date back to the beginning of the industrial revolution, but environmental awareness on a global scale gained importance after the second quarter of the 20th century (7, 17–19). Heavy metal pollution is one of the main environmental problems caused by industrialization (7, 8, 28, 29, 20–27). In addition, radioactive exposures were added to heavy metal pollution in the following years (13, 30). The fact that environmental problems are not only caused by humans began to attract more attention after the second half of the 20th century, and studies on investigating natural environmental problems have continued increasingly after this period (30–34). Subsequently, the concept of medical geology entered the literature since the 1980s (8, 31). Natural radiation to which living things are exposed due to the geological, geochemical and physicochemical properties of the environment in which they live has an important place (13, 15, 16, 30, 32, 35–38). All living things, especially humans, even inanimate objects, are constantly exposed to radiation at varying rates, depending on the location and geological/geochemical characteristics of the environment they live in. The most important source of this natural radiation we are exposed to is radioactive elements such as uranium, thorium, potassium etc. in the structure of the earth. The tools and equipment offered by technology create human-induced artificial radiation. Artificial radiation exposure is on the social agenda as a radiological danger day by day. Although radiation exposure due to telecommunication technologies has always been on the agenda in a remarkable way in the century we live in, the most important human-induced artificial radiation danger arises from nuclear reactor accidents and nuclear weapon tests. Their devastating effects are observed during and after accidents. However, recent studies show that nearly 80% of the total radiation exposure is from natural radio isotope sources (39–41). Known important natural radiation sources are  $^{238}\text{U}$ ,  $^{232}\text{Th}$  and  $^{40}\text{K}$  radio isotopes and their decay products. Living things are exposed to the radiation of these elements through the soil they live in. Human beings continue their vital activities on this relatively thin layer of the earth's crust, especially their agricultural activities and, in most cases, they establish their settlement areas on this part of the earth's crust. Geological effects and climate are undeniably important in the physicochemical, geochemical, mineralogy and petrological properties of the soil bedrock. The elemental contents of the rock are transferred to the soil to a greater or lesser extent during the soil formation process. Among these elements that pass from the rocks to the soil, the origin of natural radioactivity in the soil are  $^{238}\text{U}$  (99.27% of uranium),  $^{235}\text{U}$  (0.72% of uranium),  $^{232}\text{Th}$  (100% of thorium) and  $^{40}\text{K}$  (0.012% of potassium), which have long

half-lives. are the decay products of radioisotopes (41, 42). These radioisotopes are the main sources of external and internal radiation doses to which all living things, people and objects are exposed. The most important source of internal radiation includes reaching the atmospheric environment from soil and rocks and eventually reaching humans through the inhalation of the  $^{222}\text{Rn}$  (radon) radio isotope and its decay products and/or through the direct and indirect effects of the food chain, starting from the bottom link of the food chain from soil and/or water. The Rn element spreads easily through the decay of radium (Ra) in rocks (especially as the decay product of Ra, the decay product of uranium, which is abundant in granitic rocks) (40–43). External radiation originates from gamma-decaying radioisotopes in the uranium and thorium series and from the naturally occurring radioisotope potassium-40 ( $^{40}\text{K}$ ), which is not the decay product of any radioactive heavy metal. In addition to its long half-life,  $^{40}\text{K}$  is as dangerous as  $^{226}\text{Ra}$  in terms of radioactive exposure, especially because it is abundant in rocks close to the surface.

When human-made radio isotopes are mentioned, the first and most dangerous ones that come to mind are the radio isotopes such as  $^{137}\text{Cs}$ ,  $^{131}\text{I}$ ,  $^{95}\text{Zr}$  and  $^{90}\text{Sr}$ , which occur during nuclear power plant accidents or nuclear weapons tests. The most dangerous and important of these isotopes is the  $^{137}\text{Cs}$  radioisotope. For example, it is estimated that 70 PBq of  $^{137}\text{Cs}$  and 330 PBq of  $^{131}\text{I}$  were released into the atmosphere in the first ten-day period due to the Chernobyl nuclear power plant accident (44, 45). Due to the effect of winds that were active in many directions during the ten days of this release, radioactive materials spread over a wide area in the northern hemisphere, especially in Europe, in Ukraine and the nearby region where the accident occurred. While the effect of  $^{131}\text{I}$  was effective in the early days of the accident and in nearby areas due to the short half-life of the element, the effect of  $^{134}\text{Cs}$  and  $^{137}\text{Cs}$  radioisotopes with longer half-lives had the opportunity to spread to many important parts of the exposed body and was effective for many years (45–47). Observation of these artificial radio nuclei of nuclear origin is useful in investigating the environmental effects of nuclear power plants and nuclear tests. In this context,  $^{137}\text{Cs}$  radio isotopes with a half-life of 30.2 years are particularly preferred. In the light of the above explanations, it can be said that people who stay in an environment where natural or artificial radiation is present for a long-time face risks of excessive radiation exposure. Especially in recent years, research indicates that granitic rocks have natural radionuclide concentrations (38, 48, 49). Table 1 delineates the concentrations of potassium (K), uranium (U), and thorium (Th) across diverse geological environments. The assessment of natural radiation levels within the environment or material is predominantly conducted through the widespread application of gamma-ray spectrometry. Complementary to this method, empirical approaches are employed to ascertain the natural radiation level (38, 50–52).

Gümüşhane is situated in the Eastern Blacksea region, one of Türkiye's important metallogenic belts. Gümüşhane has many mines currently operating. For this reason, there are many scientific studies on geology-mineral geology in the region (53–60). Karamustafa gold-bearing Zn-Pb-(±Cu) deposit is one of the important mineral deposits currently being operated in the region. In this study, it was aimed to investigate the natural and artificial radiation contents of the soil in the Karamustafa mining area.

## 2. MATERIAL AND METHODS

### 2.1. General Geology of the Area

Karamustafa gold-bearing Zn-Pb mine, which is the subject of the study, is located 35 km southwest of Gümüşhane City center (Fig. 1). The mine site is in the southern zone of the Eastern Pontides metallogenic belt. The study area covers an area of approximately 4 km<sup>2</sup>. The oldest unit of the mine area and its immediate surroundings is the Late to Early Carboniferous aged Gümüşhane pluton (granitoid) (53, 58, 61–64). This pluton is unconformably overlain by the Zimonköy formation, which has a volcano-sedimentary character and is of Early-Middle Jurassic age (65, 66). Zimonköy formation are overlain by the Berdiga formation, consisting of Late Jurassic-Early Cretaceous

limestones (67). Kermutdere formation (68, 69) lie unconformably on the Berdiga formation and consist of clastic and, in some areas, volcanic-clastic units. This formation is cut by Late Cretaceous plutons around Torul (70, 71). Kermutdere formation is overlain by the Eocene aged Alibaba formation, which consists of mainly volcanic and a small extent of sedimentary rocks unconformably in different parts of the region (54, 72–74). These units are cut by contemporaneous calc-alkaline granitic plutons in different places (57, 75–78). The youngest units in the mine area and its surroundings are Quaternary alluviums and travertines (79, 80).

**Table 1. Concentration of K, U and Th radioactive elements ( in ppm) and the ratios of Th/U and K/U in the Earth's parts (81)**

	K	U	Th	Th/U	K/U
Continental crust	27.500	2,5	10,5	4,20	11.000
Upper					
Middle(Archaeon)	17.500	2,2	8,4	3,82	7.954
Lower(Archaeon)	8.333	0,05	0,42	8,40	166.660
Lower and Middle (post Archaeon)	20.000	1,25	6	4,80	16.000
Average (1)	17.500	1,3	5,7	4,38	13.461
Average (2)	12.500	1,25	4,80	3,84	10.000
Oceanic crust	600	0,047	0,12	2,55	12.766
Normal Mid-Ocean Ridge Basalt (NMORB)					
Ocean Island Basalt (OIB)	12.000	1,02	4	3,92	11.765
CI Carbonaceous chondrites	545	0,0074	0,029	3,92	73.649
Primitive mantle	250	0,021	0,085	4,05	11.905
Bulk silicate earth	240	0,023	0,0795	3,46	10.435

## 2.2. Collection, preparation and radioactive measurements of the samples

To ascertain the radioactivity values within the mining locales, a total of nine samples were collected from the Karamustafa mine area. The selection of sample locations and the number of samples to be taken were based on the general geological features of the study area, the alteration, and the mineralization characteristics. The International Organization for Standardization (ISO) 11929-1:2017 standard is used for the collection of soil samples for the detection of natural radiation. This standard defines the procedures and requirements for the collection, transportation, and storage of soil samples (82). The samples were taken from outside the agricultural areas, by cleaning the area around the sampling point so as not to contain organic matter, and from the B level of the soil section, from a depth of 0-15 cm from the surface, and were kept at room temperature for an average of 10 days to remove their natural moisture. After the dried samples were passed through 2 mm teflon sieves, they were transferred to tared marinelli counting containers. The weight of each sample was weighed and recorded, and the lids of each container were tightly locked to prevent air from entering from the outside. The samples were kept in the laboratory in a suitable environment for 1 month in order for the degradation products in the soil to come into radioactive balance with  $^{238}\text{U}$  and  $^{232}\text{Th}$  (83), and then their analysis was carried out using a gamma-ray spectrometer at the Gümüşhane University Central Laboratory (Gümüşhane, Türkiye).

When determining external irradiation gamma radioactivity levels, it is important to place the detector and sample according to the most appropriate counting geometry. For this purpose, marinelli containers are preferred because they provide high efficiency. The shapes and sizes of Marinelli containers vary depending on the detector dimensions and the amount of sample that can be supplied. In the layout geometry, when the detector is located in the space in the middle of the Marinelli container, it is surrounded by the sample and the efficiency is increased by allowing more gamma rays to reach the detector. In low-level radioactivity measurements, the use of semiconductor detectors and scintillation detectors is common. The biggest advantage of semiconductor detectors is their very good energy separation power. In this way, peaks that are very close to each other can be

easily distinguished. Germanium and silicon are mostly used in the construction of solid state detectors. In solid state detectors, incoming radiation interacts with the crystal and loses its energy. As a result of these interactions, high-energy electrons removed from crystal atoms interact with other electrons and form ion pairs, and the event becomes stable in a very short time, approximately 10-12 seconds. This accumulated charge is dragged along the crystal by an externally applied electric field and an electrical signal is obtained. The amount of charge generated within the crystal and collected on the contact surfaces is only proportional to the absorbed energy, regardless of the type of radiation. The energy required to form an electron pair is around 3eV in semiconductors, 30eV in gas ionization chambers and 300eV in scintillation detectors. Photons with energies between 1keV and 60keV are measured with Si(Li) detectors, and those with energies between 5keV and 10Mev are measured with Ge(Li) or pure Ge(HPGe) detectors. All three detectors operate at liquid nitrogen temperature (77° K) because the lithium atoms embedded in Si and Ge crystals are very mobile at high temperatures. As mentioned above, a Popton Ortec detector was used in our study.

### 2.3. Radiation Indices

The effects of both artificial and natural radiation on humans and the environment are evaluated using different indices and parameters. In this study, absorbed dose rate (D), annual effective dose rate (AEDR), radium equivalent activity ( $R_{aeq}$ ), external hazard index ( $H_{ex}$ ) and internal hazard index ( $H_{in}$ ) were used.

#### 2.3.1. Absorbed Dose Rate (D)

The risk associated with natural radionuclides in soil is usually expressed in terms of the absorbed dose rate (D) (nanoGray/hour, nGy/h) or exposure rate in air at 1 meter above the surface. Generally, the  $^{137}\text{Cs}$  and  $^{90}\text{Sr}$  artificial radio nuclei (radio isotopes) and the  $^{235}\text{U}$  decay series can be neglected. Therefore, since natural radioactivity consists mainly of Th, Ra and K radio isotopes, it may be useful to calculate absorbed dose rates based on these (43, 46, 84). In the calculation of the absorbed dose rate, average specific activity coefficients of 0.462 for U (in Ra), 0.604 for Th and 0.0417 for K' in the soil are used. In cases where  $^{137}\text{Cs}$  is taken into account, this coefficient for  $^{137}\text{Cs}$  is 0.1125 (nGy/h in Bq/kg) (41, 84, 85). Absorbed dose rate is calculated by the formula below.

$$D(\text{nGy/h}) = 0.462A_{226\text{Ra}} + 0.604A_{232\text{Th}} + 0.0417A_{40\text{K}} \quad (1a)$$

If the effect of artificial radio isotopes of human origin is also in question, then the formula is as follows (86).

$$D(\text{nGy/h}) = 0.462A_{226\text{Ra}} + 0.604A_{232\text{Th}} + 0.0417A_{40\text{K}} + 0.112A_{137\text{Cs}} \quad (1b)$$

In the formulas, D corresponds to the absorbed dose rate and its unit is nanoGray/hour (nGy/h). In natural environment radioactivity situations, the annual effective dose is calculated by multiplying the absorbed dose (40) value and the factor  $0.69 \text{ Sv Gy}^{-1}$ .  $A_{226\text{Ra}}$ ,  $A_{232\text{Th}}$ ,  $A_{40\text{K}}$  ve  $A_{137\text{Cs}}$  in the formulas refer to the activity concentrations of  $^{226}\text{Ra}$ ,  $^{232}\text{Th}$ ,  $^{40}\text{K}$  and  $^{137}\text{Cs}$ , respectively. World averages for absorbed dose rate were calculated as 51 nGy/h based on the median values of world Ra, Th and K activities (46).

#### 2.3.2. Annual Effective Dose Rate (AEDR)

One of the most frequently used parameters is the Annual Effective Dose Rate (AEDR). From the absorbed dose rate in air, the effective dose received by humans is calculated using the relevant coefficients. This parameter is used to protect against potential biological effects and radiation associated with exposure to ionizing radiation in humans. The annual effective dose rate from natural terrestrial nuclei is sometimes expressed as the natural annual effective dose rate (AEDR<sub>nat</sub>) or the terrestrial annual effective dose rate (AEDR<sub>ter</sub>) and is calculated by the formula below (84):

$$AEDR_{nat}=0.69*D*[(1-I_{in})+SF.I_{in}]*24*365.25*10^{-3} \quad (2)$$

In the formula,  $I_{in}$  (0.8) represents the indoor dose exposure factor and SF represents the protection factor (0.2). The coefficient of 0.69 is the factor for converting the absorbed dose in air into the human effective dose for adults ( $SvGy^{-1}$ ).

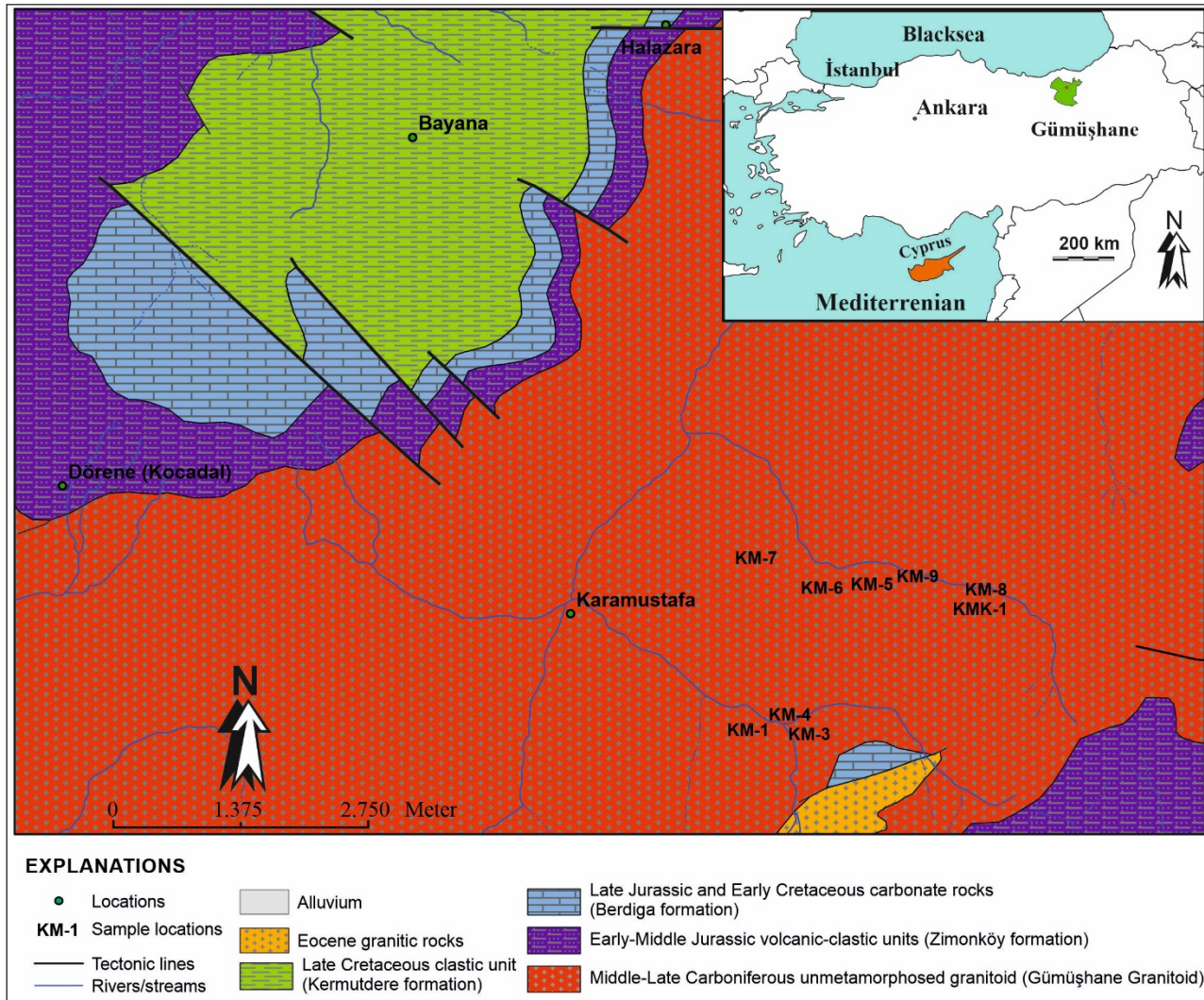


**Figure 1. Study sites location map and general geological map of the Karamustafa gold bearing Zn-Pb mine site and its near vicinity (after (87))**

### 2.3.3. Radiation hazard indices

Different indices are used to determine the environmental effects of natural and artificial radiation. Among these, the External (external) radiation hazard index ( $H_{ex}$ ) was proposed by Krieger (1981) and expresses the risk associated with the external source of gamma rays. The external (external) radiation hazard index is accepted as the allowable dose for the public as 1 mSv/year. In soil,  $H_{ex}$  is calculated by the following formula:

$$H_{ex} = \frac{A_{226Ra}}{370} + \frac{A_{232Th}}{259} + \frac{A_{40K}}{4810} \quad (3)$$

In the formula, the parameters  $A_{226Ra}, A_{232Th}, A_{40K}$  represent the Bq/kg activity concentrations of  $^{226}Ra, ^{232}Th$  and  $^{40}K$ . If the extrinsic (external) hazard index  $H_{ex} > 1$ , it indicates that the external dose to which humans are exposed has exceeded the acceptable level (38, 84).

The internal radiation hazard index ( $H_{in}$ ) is calculated by the following equation.

$$H_{in} = \frac{A_{226Ra}}{185} + \frac{A_{232Th}}{259} + \frac{A_{40K}}{4810} \quad (4)$$

The parameters in this formula are the same as those given in formula number 3. To avoid radiation hazards to the respiratory organs, the internal radiation hazard index ( $H_{in}$ ) should also be less than one (<1) (84).

The effect of all radio nuclei on the potential radiation is also calculated as the radium conjugate activity ( $Ra_{eq}$ ) (89). The radium conjugate activity ( $Ra_{eq}$ ) of the soil is calculated with the following formula, assuming that  $^{226}Ra$  is 370 Bq/kg,  $^{232}Th$  is 259 Bq/kg and  $^{40}K$  is 4810 Bq/kg.

$$Ra_{eq(ex)} \text{ (Bq/kg)} = A_{226Ra} + 1.429A_{232Th} + 0.077A_{40K} \quad (5)$$

in the formula,  $A_{226Ra}$ ,  $A_{232Th}$ ,  $A_{40K}$  refer to the activity concentrations of  $^{226}Ra$ ,  $^{232}Th$  and  $^{40}K$ , respectively. The threshold value for  $Ra_{eq}$  value is 370 Bq/kg. When this threshold value is exceeded for the measured material/environment, the material/environment is considered to have a hazardous potential.

### 3. RESULTS AND DISCUSSIONS

#### 3.1. Natural and artificial radio isotope activities

Within the scope of the study, the natural radioactivity of  $^{232}Th$ ,  $^{226}Ra$  and  $^{40}K$  radio isotopes and the artificial radioactivity of  $^{137}Cs$  of the soil samples taken from the Karamustafa gold bearing Zn-Pb-(±Cu) mining area were measured and are given in Table 2.

**Table 2. Mine Site Natural radioactivity levels for Th, Ra, K and Cs elements. (in value±standard deviation) (Bold fonts in the table indicate that the world weighted average for the relevant radio isotope is exceeded)**

Samples	$^{232}Th$	$^{226}Ra$	$^{40}K$	$^{137}Cs$
Sample-1	36±1,22	16,3±0,34	<b>476±1,64</b>	1±0,01
Sample -2	<b>54±1,47</b>	13±0,38	<b>643,28±2,28</b>	0
Sample -3	<b>66±1,78</b>	<b>56±1,54</b>	<b>722,43±2,38</b>	0
Sample -4	<b>72±1,49</b>	<b>46,3±1,16</b>	<b>622±2,13</b>	2±0,02
Sample -5	36±1,23	17,9±0,36	<b>543±1,43</b>	2±0,01
Sample -6	24±1,34	23,5±0,56	<b>498±1,86</b>	4±0,02
Sample -7	19±1,03	<b>35,6±1,76</b>	<b>587±1,82</b>	6±0,03
Sample -8	13±0,86	<b>41,5±1,84</b>	398±1,56	6±0,02
Sample -9	17±0,95	27,9±0,94	397±1,73	4±0,01
Minimum	13	13	397	0
Maximum	72	56	722,43	6
Average	37,44	30,89	542,97	2,78
Geometric Mean	31,83	27,68	532,64	
Standard Deviation	20,61	14,02	105,03	2,20
<b>UNSCEAR (2000)</b>	<b>45</b>	<b>32</b>	<b>420</b>	-

\* Arithmetic means calculated without taking into account standard errors

It was determined that the natural radioactivity  $^{232}Th$  activity concentrations of Karamustafa gold bearing Zn-Pb mining area soils varied between 13±0.86 and 72±1.49 Bq/kg, and the average  $^{232}Th$  value was 37.44±20.61 Bq/kg. It was determined that  $^{226}Ra$  values varied between 13±0.38 and 56±1.54 Bq/kg, and the average  $^{226}Ra$  value was 30.89±14.02 Bq/kg. It was determined that  $^{40}K$  values varied between 397±1.73 and 722.43±2.38 Bq/kg, and the average  $^{40}K$  value was 542.97±105.03 Bq/kg. It was determined that the artificial radioisotope  $^{137}Cs$  radioactivity values were below the detection limit at two sampling points, and varied between 1±0.01 and 6±0.03 Bq/kg at other points, and the average  $^{137}Cs$  activity was 2.78±2.20 Bq/kg (Table 2, Figure 2). According to

the UNSCEAR (2000) report, the weighted world average of  $^{232}\text{Th}$ ,  $^{226}\text{Ra}$  and  $^{40}\text{K}$  activity concentrations in the earth's crust are given as 45, 32 and 420 Bq/kg, respectively. Considering these threshold values, it was observed that  $^{232}\text{Th}$  radio isotope activity concentrations exceeded the threshold value at 3 sampling points in the study area. Considering the  $^{226}\text{Ra}$  radio isotope activity concentrations, it was observed that the threshold value for  $^{226}\text{Ra}$ , 32 Bq/kg, was exceeded at 4 sampling points. When the mining area was evaluated in terms of  $^{40}\text{K}$ , it was seen that the threshold value of 420 Bq/kg was exceeded at all sampling points except 2 sampling points. Considering that the global average value of  $^{40}\text{K}$  reported by Chandrasankaran et al., (90) and Sartandel et al., (91) is 400 Bq/kg, it can be said that the  $^{40}\text{K}$  values at almost all sample points exceed the global average value. (A threshold value of 35 for Th was suggested by the same authors). While the mining area is normally expected to be low and/or below the detection limit in terms of the artificial radio isotope  $^{137}\text{Cs}$ ,  $^{137}\text{Cs}$  values above the detection limit were detected at all sampling points except 2 sampling points (Table 2, Figure 2).

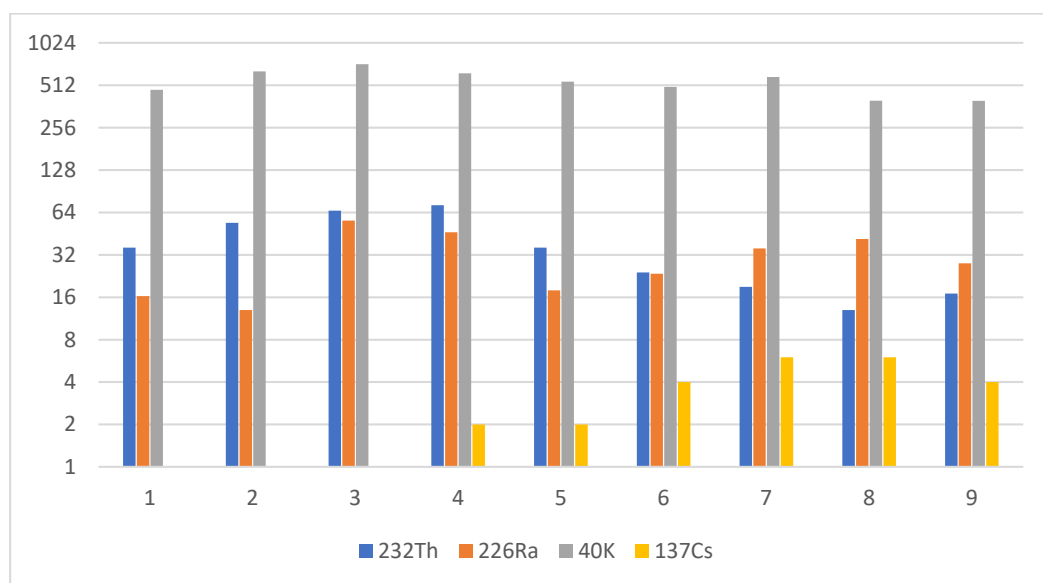


**Figure 2. Bar chart of natural and artificial radioactivity levels for the elements  $^{232}\text{Th}$ ,  $^{226}\text{Ra}$ ,  $^{40}\text{K}$  and  $^{137}\text{Cs}$  in the Karamustafa gold bearing Zn-Pb Mine field**

Radiation risks related to the  $^{137}\text{Cs}$  radio isotope occur due to human-induced activities, as mentioned above, and the most important environmental risks occur mostly in relation to nuclear power plant accidents and/or nuclear weapons tests and similar processes that are contrary to the normal flow of life. The most serious nuclear power plant accidents ever known are the Chernobyl nuclear power plant accidents in 1986 and the Fukushima nuclear power plant accidents in 2011. Immediately after the Chernobyl nuclear power plant accident, the nuclear fallout cloud spread over a wide geography, affecting the northern hemisphere, especially Europe. Many countries in Europe, including Türkiye, were affected by this radioactive fallout cloud. For example,  $^{137}\text{Cs}$  activity concentrations of 33.6 Bq/kg were measured in the soil of the Curonian Spit Forests in Lithuania. Again, in NE Lithuania, activation concentrations of 4.8-8.4 Bq/kg were recorded in the Ignalina nuclear power plant area (47). Studies conducted after the Fukushima nuclear power plant accident showed that many anthropogenic radio isotopes, including radio-cesium, were released into the atmosphere, and that buildings, soils, many other materials and even people in almost every part of the earth in the eastern part of Japan were affected by these radioactive fallout (92). Like the Chernobyl accident, the northern hemisphere was directly or indirectly affected after the Fukushima accident (39). While the high concentration of  $^{137}\text{Cs}$  reached the west of North America on March 17, 2011, the first air mass containing a relatively lower concentration of  $^{137}\text{Cs}$  reached Europe on March 22, 2011 and affected the regions where it passed as precipitation (39). Although the most significant artificial radioisotope-derived pollution has been recorded with nuclear power plant accidents,  $^{137}\text{Cs}$

activity concentrations of up to 33.21 Bq/kg have been measured in soils associated with nuclear weapons testing, for example in the Mount Rainer National Park and Satsop Nuclear Power Plant area in Washington state, where nuclear weapons tests were conducted (47).

The radioactivities of  $^{232}\text{Th}$ ,  $^{226}\text{Ra}$  and  $^{40}\text{K}$  natural radio isotopes and  $^{137}\text{Cs}$  artificial isotope activities in the Karamustafa gold bearing Zn-Pb Mine area were evaluated with different radiation hazard indices in the context of human health/medical geology (Table 3).

**Table 3. Different radiation hazard indices of Karamustafa gold bearing Zn-Pb Mine field**

Samples	Hex (Limit 1)	Hin (limit 1)	Raeq (Limit 370)	D	AEDR <sub>nat</sub>
Sample-1	0,282	0,326	104,504	49,124	106,966
Sample -2	0,377	0,413	139,861	<b>65,447</b>	<b>142,509</b>
Sample -3	0,556	0,708	206,139	<b>95,861</b>	<b>208,736</b>
Sample -4	0,532	0,658	197,298	<b>90,816</b>	<b>197,750</b>
Sample -5	0,300	0,349	111,263	<b>52,657</b>	<b>114,659</b>
Sample -6	0,260	0,323	96,214	46,120	100,424
Sample -7	0,292	0,388	108,007	<b>52,401</b>	<b>114,102</b>
Sample -8	0,245	0,357	90,762	43,622	94,985
Sample -9	0,224	0,299	82,813	39,713	86,473
Minimum	0,224	0,299	82,813	39,713	86,473
Maximum	0,556	0,708	206,139	<b>95,861</b>	208,736
Average	0,341	0,424	126,318	<b>59,529</b>	129,623
Geometric Mean	0,324	0,405	120,016	<b>56,817</b>	123,717
Standard Deviation	0,116	0,142	43,068	19,338	42,109
<b>Limit values</b>	<b>1.00</b>	<b>1.00</b>	<b>370</b>	<b>51</b>	<b>111</b>

When the natural and artificial radioactivity values of the soils in the Karamustafa mining/mineralization area are evaluated together, it has been determined that the mineralization has developed more intensively, and therefore, in areas where the associated hydrothermal alteration development is intense, the Th, Ra and K values are close to or exceed the weighted average values recommended by (41). The fact that artificial radioactivity  $^{137}\text{Cs}$  activities were detected in the soil in the field strengthens the fact that the region was probably affected by the Chernobyl Nuclear Power Plant accident.

### 3.2. Radiation hazard indices

It was determined that the external radiation index  $H_{ex}$  values of Karamustafa gold bearing Zn-Pb±Cu mining area soils varied between 0,22 and 0,57, and the average value was 0,34 (Geo.Mean:0,32). It has been observed that the mining site does not exceed 1 (one) value in terms of  $H_{ex}$  at any of the sampling points ( $H_{ex}<1$ ), therefore, there is no action to be taken in the field in terms of the external radiation hazard index  $H_{ex}$ . It has been determined that the internal radiation index  $H_{in}$  rates of the field vary between 0,30 and 0,71, and the average value is 0,42 (Geo. Mean: 0,41).

It was calculated that the radium equivalent radiation ( $R_{aeq}$ ) values of the study area soils varied between 82,81 and 206,14 Bq/kg, and the average value was 126,32 (Geo. Mean: 120.02) Bq/kg. When evaluating the  $R_{aeq}$  values in the field and/or materials, it is taken into account whether the calculated  $R_{aeq}$  values are greater than 370 Bq/kg. So the  $R_{aeq}$  threshold value is 370 Bq/kg. It was observed that the calculated  $R_{aeq}$  values of the field did not exceed 370 Bq/kg at any sampling point (Table 3).

The absorbed dose rate (D) for Karamustafa gold bearing Zn-Pb±Cu mining area was calculated to vary between 39,71 and 95,86 nGy/h, and its arithmetic average was calculated as 59,53

(Geo. Mean: 56.82) nGy/h. It was determined that the world average absorbed dose rate (51 nGy/h) (41) was exceeded at more than half of the sampling points in the field (55%; 5 sampling points). Considering these data, it would be useful to conduct a more detailed research for the area.

Since it is planned to conduct a more detailed study later, annual effective dose rates were calculated in this study without taking  $^{137}\text{Cs}$  values into consideration. It was determined that the annual effective dose rates for the study area soils varied between 86.47 and 208.73  $\mu\text{Sv/y}$ , with an average of 129,62 (Geo. Average: 123,72)  $\mu\text{Sv/y}$ . As detailed in Ali et al., (46), world effective dose rates are calculated as 111  $\mu\text{Sv/y}$ , based on the absorbed dose rate (51 gGy/h). Considering the annual effective dose rates of the field, it is seen that the threshold value has been exceeded for points other than 4 sampling points. In terms of the annual effective dose rate for the site, both the geometric mean and the arithmetic mean value exceed the threshold value. Therefore, it is thought that it would be useful to conduct more detailed studies in the field in terms of medical geology.

When the overall region is evaluated in terms of radiogenic risk, in the study conducted by Vural (15) in the Demirören (Gümüşhane, NE Türkiye) hydrothermal alteration field in the northeast of the study area, it was determined that  $^{40}\text{K}$  and  $^{232}\text{Th}$  values exceed the recommended values (400 Bq/kg and 30 Bq/kg, respectively (90, 91)). The researchers concluded that the high natural radioactivity in the region is associated with intense hydrothermal alteration. It shows that hydrothermal processes contribute to the liberation of K, U and Th elements found in minerals in rocks. Therefore, it is seen as a strong possibility that this process is effective in the increase in natural radioactivity concentrations. Apart from this, there are also studies investigating radioactivity exposures of hydrothermal alteration and/or mineralization areas from different parts of the region (16, 35, 36, 52, 93). In the study conducted by the mentioned researchers in the Eskiköy (Gümüşhane, NE Türkiye) mineralization field, it was determined that the U and Th activities in the region exceeded the accepted global average values at some points of the mineralization field, while in terms of K activity, they stated that it generally exceeded the accepted average value in all sampled regions of the field. In these studies, they found that artificial radioactivity values ( $^{137}\text{Cs}$ ) were remarkably high (up to 3 Bq/kg). While alterations and mineralizations in natural radioactivity were found to be effective, they stated that artificial radioactivity values were of human/anthropogenic origin.

In a study conducted by Kaya et al. (93), and Vural and Kaya (30, 37) covering the Arzular-Dölek-Yitirmez (Gümüşhane, NE Türkiye) mineralization and alteration areas located in the east-northeast of Gümüşhane, the natural and artificial radioisotope activities of the relevant mineralization and alteration areas were investigated. It has been determined that  $^{232}\text{Th}$  and radioisotope activities in the fields exceed the weighted world averages at many sampling points representing the field. They determined that the natural high radioisotope activities in the field triggered hydrothermal alteration developments and mineralization processes affecting the lithological units in the region. It has also been determined that artificial radioisotope activity in the region has reached remarkable levels (in some places  $> 2$  Bq/kg). Studies on granitic rocks in the region also indicate the existence of natural radioisotope activities that have reached remarkable levels.

#### 4. CONCLUSION

When Karamustafa gold bearing Zn-Pb-( $\pm$ Cu) mine field data and studies in the region in general are evaluated together, in the mining area subject to the study, especially the points where intense alteration is seen and/or mineralization areas are risky areas in terms of natural radioactivity, especially for K and Ra elements, and in terms of Th natural radioactivity values. It can be said that there are areas that need to be approached with caution. High Cs values were thought to be a sign that the region was affected by the Chernobyl disaster in 1986. The fact that the areas with significant radiation levels are located outside of residential areas is an advantage. However, it is important to consider the natural and artificial radiation levels in the area when planning environmental

remediation activities after mining activities in the region. Based on the results of detailed radiation studies, additional remediation activities should be planned if necessary.

### Funding

This study was supported by Gümüşhane University Scientific Research Coordination Office (Project No: 17.F5120.02.01)

### Conflict of interests

The authors declared no conflict of interest regarding this study.

### Acknowledgments

The author thanks to GÜBAP for its support. The authors also thank Prof. Dr. Necati Çelik (Gümüşhane University) for his support in determining radioisotope activities.

### REFERENCES

1. Vural A, Kaya S, Başaran N, Songören OT (2009) Anadolu Madencilğinde İlk Adımlar. Ankara, Türkiye, Maden Tetkik ve Arama Genel Müdürlüğü, MTA Kültür Serisi-3.
2. Vural A, Ünlü T (2020) The geology and mineralogical/petrographic features of Umurbabadağ and its surroundings (Eşme, Uşak - Turkey ). *Journal of Engineering Research and Applied Science* 9:1561–1587.
3. Eriş H (2019) The Swot Analysis For Health Tourism of Şanlıurfa. *Electronic Journal of Social Sciences* 71:1278–1298.
4. Eriş H, Barut S (2020) Sağlık Turizmi. In: Eriş H (ed), Sağlık Turizmi, Ankara, Türkiye, İKSAD, pp 45–60.
5. Eriş H, Kemer E (2020) Medical Tourism Awareness of Health Workers. *Medico-legal Update* 20:38–43.
6. Eriş H (2020) Sağlık Turizmi. 1st Ed. Ankara, Türkiye, İKSAD.
7. Vural A (2014) Trace/heavy metal accumulation in soil and in the shoots of acacia tree, Gümüşhane-Turkey. *Bulletin of the Mineral Research and Exploration* 148:85–106.
8. Vural A (2018) Demirören (Gümüşhane) ve Çevre Kayaçlarının Element İçeriklerinin Tıbbi Jeoloji Açısından İncelenmesi. 71. Türkiye Jeoloji Kurultayı, Ankara, Türkiye, Türkiye Jeoloji Kurultayı, pp 885–886.
9. Vural A (2016) Assessment of Sessile Oak (*Quercus petraea* L.) Leaf as Bioindicator for Exploration Geochemistry. *Acta Physica Polonica A* 130:191–193.
10. Vural A (2018) Relationship between the geological environment and element accumulation capacity of *Helichrysum arenarium*. *Arabian Journal of Geosciences* 11:258.
11. Higgy RH, Pimpl M (1998) Natural and man-made radioactivity in soils and plants around the research reactor of Inshass. *Applied Radiation and Isotopes* 49:1709–1712.
12. Miah FK, Roy S, Touhiduzzaman M, Alam B (1998) Distribution of Radionuclides in soil samples in and around Dhaka city. *Applied Radiation and Isotopes* 49:133–137.
13. Vural A, Kaya A (2020) Study on the natural and artificial radioactivity risk of the Aktutan alteration site (Gümüşhane). 5.Uluslararası Sağlık Bilimleri ve Yönetimi Kongresi, Kırşehir, Türkiye.
14. Kaya S, Kaya A, Çelik N, Kara RT, Taşkın H, Koz B (2020) Determination of the environmental natural radioactivity and mapping of natural background radioactivity of the Gumushane province, Turkey. *Journal of Radioanalytical and Nuclear Chemistry* 326:933–957.
15. Vural A (2019) Investigation of the radiation risk to the inhabitants in the region close to the hydrothermal alteration site, Gümüşhane/Turkey. *Journal of Engineering Research and Applied Science* 8:1168–1176.
16. Vural A, Kaya A (2021) Eskiköy Maden Sahasının (Gümüşhane, Türkiye) Doğal (226Ra, 232Th ve 40K) ve yapay (138Cs) Radyoaktivitelerine Bulgularına Ait İlk değerlendirmeler. *Euroasia Journal of Mathematics, Engineering, Natural & Medical Sciences* 8:133–150.
17. Çiftçi A, Vural A, Ural MN (2021) Analysis of Some Concepts Related to the Environment and Health with the N-Gram Method. *Journal of International Health Sciences and Management* 7:47–54.
18. Vural A, Çiftçi A (2021) An Analysis of Some Concepts Related to Environmental Issues and Development by N-Gram. *Euroasia Journal of Social Sciences & Humanities* 8:18–28.
19. Vural A, Ural N, Çiftçi A (2020) Değerli Metallerin Sosyal / Siyasal / Ekonomik Olaylarla İlişkinin N- gram Yöntemi İle Değerlendirilmesi. *Social Mentality and Research Thinkers Journal* 6:247–257.
20. Vural A, Şahin E (2012) Gümüşhane Şehir Merkezinden Geçen Karayolunda Ağır Metal Kirliliğine Ait İlk Bulgular. *Gümüşhane Üniversitesi, Fen Bilimleri Enstitüsü Dergisi* 2:21–35.
21. Vural A (2013) Assessment of Heavy Metal Accumulation in the Roadside Soil and Plants of *Robinia pseudoacacia*, in Gumushane, Northeastern Turkey. *Ekoloji* 22:1–10.
22. Vural A (2015) Contamination assessment of heavy metals associated with an alteration area: Demirören Gumushane, NE Turkey. *Journal of the Geological Society of India* 86:215–222.
23. Sungur A, Vural A, Gündoğdu A, Soylak M (2018) Gümüştüğü Köyü (Torul-Gümüşhane) Tarım Topraklarında Manganın Jeokimyasal Karakterizasyonu. *International Trace Analysis Congress (ITAC 2018/ES-AN 2018)*, Sivas,

- Türkiye, p 231.
24. Sungur A, Vural A, Gundogdu A, Soylak M (2020) Effect of antimonite mineralization area on heavy metal contents and geochemical fractions of agricultural soils in Gümüşhane Province, Turkey. *Catena* 184:104255.
  25. Vural A, Gundogdu A, Akpınar I, Baltacı C (2017) Environmental impact of Gümüşhane City, Turkey, waste area in terms of heavy metal pollution. *Natural Hazards* 88:867–890.
  26. Vural A (2023) An evaluation of elemental enrichment in rocks: in the case of Kısacık and its neighborhood (Ayvacık, Çanakkale/Türkiye). *Journal of Geography and Cartography* 6:1–20.
  27. Vural A (2023) On the elemental contents of aspen (*Populus tremula* L.) leaves grown in the mineralization area. *Journal of Geography and Cartography* 6:1–10.
  28. Vural A, Gündoğdu A, Saka F, Bulut VN (2022) Geochemical investigation of the potability of surface water in Çit Stream and related creeks in Avliyana Basin (Gümüşhane , NE Türkiye). *Turkish Journal of Analytical Chemistry* 4:44–51.
  29. Vural A, Gündoğdu A, Saka F, Bulut VN, Soylak M (2022) The Heavy Metals and Minor Elements Effects of Mineralization and Alteration Areas with Buried Ore Deposits Potential on the Surface Waters. *Journal of Investigations on Engineering & Technology* 5:21–33.
  30. Vural A, Kaya A (2021) Arzular-Yitirmez Maden/Alterasyon Sahalarının (Gümüşhane) Doğal (226Ra, 232Th ve 40K) ve Yapay (137Cs) Radyoaktivitelerinin Araştırılması. 1st International Conference of Physics, Ankara, Türkiye, pp 315–327.
  31. Vural A, Çiçek B (2020) Cevherleşme Sahasında Gelişmiş Topraklardaki Ağır Metal Kirliliği. *Düzce Üniversitesi Bilim ve Teknoloji Dergisi* 8:1533–1547.
  32. Vural A, Albayrak M (2020) Evaluation of Gördes zeolites in terms of mineralogical , geochemical and environmental effects. *Journal of Engineering Research and Applied Science* 9:1503–1520.
  33. Kırat G, Vural A (2023) Bor'un (B) Kullanım Alanları ve Çevresel Etkileri. In: Çoğun HY, Parlar İ, Üzmuş H (eds), *Doğa ve Mühendislik Bilimlerinde Güncel Tartışmalar, Bilgin Kültür Sanat Yayınları*, pp 180–190.
  34. Kaygusuz A, Vural A (2023) Eosen Yaşlı Torul (Gümüşhane/Türkiye) Volkaniklerinin Element Temel Değerlerinin Arama Jeokimyası Amaçlı Değerlendirilmesi. 3rd International Conference on Innovative Academic Studies, Konya, Türkiye, pp 191–199.
  35. Kaya A, Vural A, Çelik N (2021) Koza ve Karamustafa Madenlerinin (Gümüşhane ) Doğal (226 Ra , 232 Th ve 40K) ve Yapay (137 Cs) Radyoaktivite Konsantrasyonlarının Araştırılması (Gümüşhane). 73. Türkiye Jeoloji Kurultayı, Ankara, Türkiye, Türkiye Jeoloji Kurultayı, pp 996–1001.
  36. Kaya A, Vural A (2020) Investigation of Natural (226Ra, 232Th and 40K) and Artificial (137Cs) Radioactivity Concentrations of Kırkpavli and Hazine Mağara Ore Deposits (Gümüşhane). 5.Uluslararası Sağlık Bilimleri ve Yönetimi Kongresi, Kırşehir, Türkiye.
  37. Vural A, Kaya A (2021) Arzular-Yitirmez-Dölek (Gümüşhane) Maden/Alterasyon Sahalarındaki Doğal (226Ra, 232Th ve 40K) ve yapay (138Cs) Radyoaktivitelerine ait ilk değerlendirmeler. *Euroasia Journal of Mathematics, Engineering, Natural & Medical Sciences* 8:105–120.
  38. Vural A (2022) The Risk of Exposure to Natural Radiations Induced Hydrothermal Alteration Sites: Case of Canca Site (Gümüşhane, Türkiye). *Göbeklitepe International Journal of Medical Sciences* 5:14–22.
  39. Koo YH, Yang YS, Song KW (2014) Radioactivity release from the Fukushima accident and its consequences: A review. *Progress in Nuclear Energy* 74:61–70.
  40. UNSCEAR (2008) United Nations Scientific Committee on the Effects of Atomic Radiation Report to the general assembly, with scientific annexes.
  41. UNSCEAR (2000) Sources, Effects and Risks of Ionizing Radiations. New York.
  42. Kaniu MI, Angeyo KH, Darby IG (2018) Occurrence and multivariate exploratory analysis of the natural radioactivity anomaly in the south coastal region of Kenya. *Radiation Physics and Chemistry* 146:34–41.
  43. Krane SK (2008) Introductory nuclear physics. New York, Wiley.
  44. UNSCEAR (1988) United Nations Scientific Committee on the Effects of Atomic Radiation. Sources, Effects and Risk Ionizing Radiation. Annex D: Exposures from the Chernobyl accident. United Nations, New York.
  45. Bouville A (1995) The Chernobyl Accident. *Radiation Protection Dosimetry* 60:287–293.
  46. Ali M, Wasim M, Iqbal S, Arif M, Saif F (2013) Determination of the risk associated with the natural and anthropogenic radionuclides from the soil of Skardu in Central Karakoram. *Radiation Protection Dosimetry* 156:213–222.
  47. Jasaitis D, Klima V, Pečiulienė M, Vasiliauskienė V, Konstantinova M (2020) Comparative Assessment of Radiation Background Due to Natural and Artificial Radionuclides in Soil in Specific Areas on the Territories of State of Washington (USA) and Lithuania. *Water, Air, and Soil Pollution* 231. doi:10.1007/s11270-020-04730-8.
  48. Mason B, Moore C (1982) Principles of geochemistry. Fourth. New York, Wiley.
  49. Rudnick R, Gao S (2010) Composition of the Continental Crust. In: Holland H, Turekian K (eds), *Readings of Treatise on Geochemistry*, London, England, Elsevier, pp 101–123. 2nd Ed.
  50. IEAE (1989) Construction and Use of Calibration Facilities for Radiometric Field Equipment. Vienna.
  51. Omeje M, Wagiran H, Ibrahim N, Lee SK, Sabris S (2013) Comparison of Activity Concentration of 238U, 232Th

- and 40K in different Layers of Subsurface Structures in Dei-Dei and Kubwa, Abuja Northcentral Nigeria. *Radiation Physics and Chemistry* 91:70–80.
52. Kaya A, Vural A, Çelik N (2021) Investigation of Natural (226Ra, 232Th and 40K) and Artificial (137Cs) Radioactivity Concentrations of Koza and Karamustafa Ore Deposits (Gümüşhane). 73rd Geological Congress of Turkey, Ankara, Türkiye, Türkiye Jeoloji Kurultayı, pp 996–1001.
  53. Vural A, Erdoğan M (2014) Eski Gümüşhane Kırkpavli Alterasyon Sahasında Toprak Jeokimyası. *Gümüşhane Üniversitesi Fen Bilimleri Enstitüsü Dergisi* 4:1–15.
  54. Vural A, Erşen F (2019) Geology, mineralogy and geochemistry of manganese mineralization in Gumushane, Turkey. *Journal of Engineering Research and Applied Science* 8:1051–1059.
  55. Vural A, Akpınar İ, Sipahi F (2021) Mineralogical and Chemical Characteristics of Clay Areas, Gümüşhane Region (NE Turkey), and Their Detection Using the Crösta Technique with Landsat 7 and 8 Images. *Natural Resources Research* 30:3955–3985.
  56. Vural A, Akpınar İ, Kaygusuz A (2021) Petrological characteristics of Cretaceous volcanic rocks of Demirören (Gümüşhane, NE Turkey) region. *Journal of Engineering Research and Applied Science* 10:1828–1842.
  57. Vural A, Kaygusuz A (2021) Geochronology, petrogenesis and tectonic importance of Eocene I-type magmatism in the Eastern Pontides, NE Turkey. *Arabian Journal of Geosciences* 14:467.
  58. Vural A, Kaygusuz A (2019) Petrology of the Paleozoic Plutons in Eastern Pontides: Artabel Pluton (Gümüşhane, NE Turkey). *Journal of Engineering Research and Applied Science* 8:1216–1228.
  59. Lermi A (2003) Midi (Karamustafa/Gümüşhane, KD Türkiye) Zn-Pb Yatağının Jeolojik, Mineralojik, Jeokimyasal ve Kökensel İncelemesi. Dissertation, K.T.Ü. Trabzon, Türkiye.
  60. Sipahi F, Saydam Eker Ç, Akpınar İ, Gücer MA, Vural A, Kaygusuz A, Aydurmuş T (2022) Eocene magmatism and associated Fe-Cu mineralization in northeastern Turkey: a case study of the Karadağ skarn. *International Geology Review* 64:1530–1555.
  61. Yılmaz Y (1972) Petrology and structure of the Gümüşhane granite and surrounding rocks, NE Anatolia.
  62. Vural A (2019) Evaluation of soil geochemistry data of Canca Area (Gümüşhane, Turkey) by means of Inverse Distance Weighting (IDW) and Kriging methods-preliminary findings. *Bulletin of the Mineral Research and Exploration* 158:195–216.
  63. Kaygusuz A, Arslan M, Siebel W, Sipahi F, Ilbeyli N (2012) Geochronological evidence and tectonic significance of Carboniferous magmatism in the southwest Trabzon area, eastern Pontides, Turkey. *International Geology Review* 54:1776–1800.
  64. Kaygusuz A (2020) Geochronological age relationships of Carboniferous Plutons in the Eastern Pontides ( NE Turkey ). *Journal of Engineering Research and Applied Science* 9:1299–1307.
  65. Eren M (1983) Gümüşhane-Kale Arasının Jeolojisi ve Mikrofasiyes incelemeesi. Dissertation, Karadeniz Teknik Üniversitesi.
  66. Saydam Eker C, Sipahi F, Kaygusuz A (2012) Trace and Rare Earth Elements as Indicators of Provenance and Depositional Environments of Lias Cherts in Gumushane, NE, Turkey,. *Chemie der Erde - Geochemistry* 72:167–177.
  67. Pelin S (1977) Alucra (Giresun) Güneydoğu Yöresinin Petrol Olanakları Bakımından Jeolojik İncelenmesi. *Karadeniz Teknik Üniversitesi Yayınları*:87–103.
  68. Tokel S (1972) Stratigraphical and volcanic history of Gümüşhane region.
  69. Saydam Eker C, Korkmaz S (2011) Mineralogy and whole rock geochemistry of late Cretaceous sandstones from the eastern Pontides (NE Turkey). *Neues Jahrbuch für Mineralogie, Abhandlungen* 188:235–256.
  70. Kaygusuz A, Siebel W, Şen C, Satir M (2008) Petrochemistry and petrology of I-type granitoids in an arc setting: The composite Torul pluton, Eastern Pontides, NE Turkey. *International Journal of Earth Sciences* 97:739–764.
  71. Kaygusuz A, Siebel W, Ilbeyli N, Arslan M, Satir M, Şen C (2010) Insight into magma genesis at convergent plate margins – a case study from the eastern Pontides (NE Turkey). *Neues Jahrbuch für Mineralogie - Abhandlungen* 187:265–287.
  72. Kaygusuz A, Arslan A, Siebel W, Şen C (2011) Geochemical and Sr-Nd Isotopic Characteristics of Post-Collisional Calc-Alkaline Volcanics in the Eastern Pontides (NE Turkey). *Turkish Journal of Earth Sciences* 20:137–159.
  73. Arslan M, Temizel İ, Abdioğlu E, Kolaylı H, Yücel C, Boztuğ D, Şen C (2013) 40Ar–39Ar dating, whole-rock and Sr–Nd–Pb isotope geochemistry of post-collisional Eocene volcanic rocks in the southern part of the Eastern Pontides (NE Turkey): implications for magma evolution in extension-induced origin. *Contributions to Mineralogy and Petrology* 166:113–142.
  74. Aslan Z, Arslan M, Temizel İ, Kaygusuz A (2014) K-Ar dating, whole-rock and Sr-Nd isotope geochemistry of calc-alkaline volcanic rocks around the Gümüşhane area: Implications for post-collisional volcanism in the Eastern Pontides, Northeast Turkey. *Mineralogy and Petrology* 108:245–267.
  75. Karlı O, Chen B, Aydın F, Şen C (2007) Geochemical and Sr-Nd-Pb isotopic compositions of the Eocene Dölek and Sariçiçek Plutons, Eastern Turkey: Implications for magma interaction in the genesis of high-K calc-alkaline granitoids in a post-collision extensional setting. *Lithos* 98:67–96.
  76. Kaygusuz A, Öztürk M (2015) Geochronology, geochemistry, and petrogenesis of the Eocene Bayburt intrusions,

- Eastern Pontide, NE Turkey: implications for lithospheric mantle and lower crustal sources in the high-K calc-alkaline magmatism. *Journal of Asian Earth Sciences* 108:97–116.
77. Kaygusuz A, Yücel C, Arslan M, Sipahi F, Temizel İ, Çakmak G, Güloğlu ZS (2018) Petrography, mineral chemistry and crystallization conditions of Cenozoic plutonic rocks located to the north of Bayburt (Eastern Pontides, Turkey). *Bulletin of the Mineral Research and Exploration* 157:75–102.
  78. Kaygusuz A, Yücel C, Arslan M, Temizel İ, Yi K, Jeong Y-J, Siebel W, Sipahi F (2020) Eocene I-type magmatism in the Eastern Pontides, NE Turkey: Insights into magma genesis and magma-tectonic evolution from whole-rock geochemistry, geochronology and isotope systematics. *International Geology Review*. doi:doi.org/10.1080/00206814.2019.1647468.
  79. Vural A (2019) Zenginleştirilmiş Jeoturizm Güzergahlarına Dair Farkındalık Oluşturulması : Eski Gümüşhane - Dörtkonak Güzergahı. *Gümüşhane Üniversitesi Sosyal Bilimler Enstitüsü Elektronik Dergisi* 10:250–274.
  80. Vural A, Külekçi G (2021) Zenginleştirilmiş Jeoturizm Güzergahı:Gümüşhane-Bahçecik Köyü. *Euroasia Journal of Mathematics, Engineering, Natural & Medical Sciences* 8:1–23.
  81. Plant JA, Simpson PR, Smith B, Windley BF (1999) Uranium ore deposits products of the radioactive Earth. *Reviews in Mineralogy* 38:255–319.
  82. ISO 11929-1:2017 (2017) International Organization for Standardization. (2017). Soil sampling for the detection of natural radiation - Part 1: General principles. ISO 11929-1:2017 Available at: <https://www.iso.org/standard/68383.html>.
  83. Chiozzi P, Pasquale V, Verdoya M (2007) Radiometric survey for exploration of hydrothermal alteration in a volcanic area. *Journal of Geochemical Exploration* 93:13–20.
  84. Ali M, Iqbal S, Wasim M, Arif M, Saif F (2013) Soil radioactivity levels and radiological risk assessment in the highlands of Hunza. Pakistan. *Radiation Protection Dosimetry* 153:390–399.
  85. Beretka J, Mathew PJ (1985) Natural Radioactivity of Australian Building Materials. *Industrial Wastes and By-Products Health Physics* 48:87–95.
  86. Ribeiro FCA, Silva JIR, Lima ESA, do Amaral Sobrinho NMB, Perez D V., Lauria DC (2018) Natural radioactivity in soils of the state of Rio de Janeiro (Brazil): Radiological characterization and relationships to geological formation, soil types and soil properties. *Journal of Environmental Radioactivity* 182:34–43.
  87. Güven İH (1993) Doğu Pontidlerin 1/100.000 Ölçekli Kompilasyonu. Ankara, MTA Genel Müdürlüğü.
  88. Krieger VR (1981) Radioactivity of construction materials. *Betonwerk Fertigteil Techn* 47:468–473.
  89. Singh S, Rani A, Mahajan RM (2005) 226Ra, 232Th and 40K analysis in soil samples from some areas of Punjab and Himachal Pradesh, India using gamma ray spectrometry. *Radiation Measurements* 39:431–439.
  90. Chandrasakaran A, Ravisankar R, Senthilkumar G, Thillaivelavan K, Dhinakaran B, Vijayagopal P, Bramha SN, Venkatraman B (2014) Spatial Distribution and Lifetime Cancer Risk due to Gamma Radioactivity in Yelagiri Hills, Tamilnadu, India. *Egyptian Journal of Basic and Applied Science* 1:38 – 48.
  91. Sartandel SJ, Jha SK, Bara SV, Tripathi RM, Puranik VD (2009) Spatial Distribution of Uranium and Thorium in the Surface Soil around Proposed Uranium Mining Site at Lambapur and its Vertical Profile in the Nagarjuna Sagar Dam. *Journal of Environmental Radioactivity* 100:831 – 834.
  92. Kato H, Onda Y, Gao X, Sanada Y, Saito K (2019) Reconstruction of a Fukushima accident-derived radiocesium fallout map for environmental transfer studies. *Journal of Environmental Radioactivity* 210:105996.
  93. Kaya A, Çelik N, Vural A (2018) Gümüşhane İlinde Maden Yataklarındaki/maden potansiyeli olan alterasyon sahalarındaki Topraktaki Doğal (226Ra, 232Th ve 40K) ve Yapay (137Cs) Radyoaktivite Konsantrasyonlarının Araştırılması. Gümüşhane, Türkiye.